Synthetic Metals 286 (2022) 117028

Contents lists available at ScienceDirect

Synthetic Metals

journal homepage: www.elsevier.com/locate/synmet

Improving stability of perovskite solar cells using fullerene-polymer composite electron transport layer

Mohamed M. Elnaggar [a,b,c], Lyubov A. Frolova [a], Alexandra M. Gordeeva [a], Marina I. Ustinova [a,d], Hannah Laurenzen [e], Alexander V. Akkuratov [a], Sergey L. Nikitenko [a], Elena A. Solov'eva [f], Sergey Yu. Luchkin [d], Yury S. Fedotov [f], Sergey A. Tsarev [d], Nadezhda N. Dremova [a], Keith J. Stevenson [d], Sergey I. Bredikhin [f], Selina Olthof [e], Sergey M. Aldoshin [a], Pavel A. Troshin [a,g,*]

[a] Institute for Problems of Chemical Physics of the Russian Academy of Sciences (IPCP RAS), Semenov prospect 1, Chernogolovka, 141432 Moscow region, Russian Federation
[b] Moscow Institute of Physics and Technology, Dolgoprudny, 141700 Moscow region, Russian Federation
[c] Department of Physics, Faculty of Science, Tanta University, 31512 Tanta, Egypt
[d] Skolkovo Institute of Science and Technology, Moscow 121205, Russian Federation
[e] Department of Chemistry, University of Cologne, Greinstrasse 4–6, 50939, Cologne, Germany
[f] Institute of Solid State Physics of RAS, Chernogolovka, Russia Federation
[g] Faculty of Chemistry, Silesian University of Technology, Strzody 9, 44-100 Gliwice, Poland

ARTICLE INFO

Keywords:
Perovskite solar cells
Conjugated polymers
Polymer/fullerene blends
Charge transport materials
P-i-n solar cell architecture

ABSTRACT

Perovskite solar cells (PSCs) have attracted significant attention due to their high efficiency and potential for low-cost manufacturing, but their commercialization is strongly impeded by low operational stability. The engineering of charge-transport layer materials have been recognized as an effective strategy to improve both stability and performance of PSCs. Here, we introduce a pyrrolo[3,4-*c*]pyrrole-1,4-dione-based n-type copolymer as an electron transport material for perovskite solar cells. Using a composite of this polymer with the fullerene derivative [60]PCBM delivered an efficiency of 16.4% and enabled long-term operational stability of p-i-n perovskite solar cells.

1. Introduction

Power conversion efficiencies (PCEs) of state-of-the-art perovskite solar cells (PSCs) have reached > 25% which is comparable to the best crystalline silicon-based solar cells [1]. Furthermore, perovskite solar cells can be produced at a low cost using scalable solution-based roll-to-roll printing and coating techniques. The main obstacle to the commercialization of PSCs is their poor operational stability [2–4]. The interfacial degradation involving charge transport layers and electrodes represents one of the common degradation pathways [5]. In particular, we showed that using the fullerene derivative [60]PCBM (phenyl C_{61} butyric acid methyl ester) as the electron transport layer (ETL) material facilitates the degradation of p-i-n perovskite solar cells [6]. Using other functional fullerene derivatives as ETL materials in PSCs could mitigate charge recombination losses and increase photovoltaic efficiency or suppress moisture-induced degradation in the air [7–9], whereas the operational stability of the devices under light exposure remains inferior. Therefore, improving the operational stability of p-i-n PSCs requires replacing fullerene-based ETLs with alternative more chemically inert materials.

In general, polymer-based semiconductors represent a very attractive family of materials for developing efficient and stable ETLs since they have excellent film formation and suppressed tendency to crystallization, so the films preserve their uniformity and do not suffer from grain boundaries effects, which is important in the context of the device stability. Furthermore, polymeric ETLs can better withstand mechanical stress induced by temperature cycling (due to different thermal expansion coefficients of different layers) and/or repeatable bending in the

* Corresponding author at: Institute for Problems of Chemical Physics of the Russian Academy of Sciences (IPCP RAS), Semenov prospect 1, Chernogolovka, 141432 Moscow region, Russian Federation
E-mail address: pavel.troshin@polsl.pl (P.A. Troshin).

https://doi.org/10.1016/j.synthmet.2022.117028
Received 2 October 2021; Received in revised form 19 January 2022; Accepted 30 January 2022
Available online 14 February 2022

case of using flexible substrates. Unfortunately, the range of available polymer-based n-type semiconductors with high electron mobility and energy levels matching the perovskite absorbers is very limited, while the design of such materials is quite challenging. Furthermore, the thermal stability of polymers could be inferior as compared to that of low molecular weight compounds [10–15].

Conjugated polymers are widely used as hole-transport materials for perovskite solar cells, whereas the number of known polymeric ETLs is very limited [16–18]. Intense research in this field over the last five years resulted in the development of a series of promising polymeric ETLs for PSCs [19–31]. However, the impact of these materials on the operational stability of PSCs is still scarcely explored. There are only two reports where the photostability of PSCs with polymeric ETLs was studied within the initial period of 1–100 h [26,31].

Herein, we introduce the conjugated polymer P1 and its composites with [60]PCBM as promising ETL materials for stabilized PSCs demonstrating the retention of > 90% and > 60% of the initial efficiency after 400 and 1200 h of continuous light exposure, respectively.

2. Results and discussion

The pyrrolo[3,4-*c*]pyrrole-1,4-dione (DPP) was chosen as a key building block to enable the optimal optoelectronic properties and high electron mobility [32], while the branched 2-butyloctyl side chains were used to achieve a good solubility[33]. To provide the desired LUMO energy of the polymer, the DPP fragment was coupled with 2,1,3-benzooxadiazole (BO) unit loaded with two glycol ether side chains for improved adhesion to the perovskite absorber [34]. The polymer P1 was synthesized *via* Stille polycondensation reaction using M1 and M2 key monomers as shown in Scheme 1 (the detailed procedure is given in Supplementary Information, SI).

The HOMO energy of P1 was estimated as − 5.11 eV, whereas the LUMO energy was found to be close to − 3.80 eV according to the cyclic voltammetry (CV) measurements (Fig. S1, Table S1, SI). UV photoelectron spectroscopy (UPS) measurements (Fig. S2, SI) performed for a thin film of P1 provided the value of 5.10 eV for the ionization energy, which is matching the electrochemistry data. Furthermore, inverse photoelectron spectroscopy (IPES) delivered an electron affinity value of 3.85 eV, which is also in good agreement with the electrochemistry data. The optical absorption spectrum and the corresponding Tauc plot (Fig. S3, SI) allowed us to estimate the optical bandgap of the polymer as 1.30 eV, which is close to the electrochemical bandgap (1.31 eV) and the bandgap value obtained from UPS and IPES (1.25 eV).

The LUMO energy of P1 is close enough to the conduction bands of $MAPbI_3$ and $Cs_{0.12}FA_{0.88}PbI_3$ and should enable a rather efficient electron extraction (Fig. 1). Unfortunately, the polymer P1 is a narrow bandgap material, therefore it cannot block holes, which might lead to recombination losses.

P1 and **P1**:[60]PCBM (1:1 w/w) blend quenched the photoluminescence (PL) of the perovskite films in a similar way as [60]PCBM did (Fig. 2). The space charge limited current (SCLC) measurements for the electron-only device architectures (ITO/Yb/active film/Ca) provided comparable electron mobilities for thin films of **P1**, [60]PCBM, and **P1**:[60]PCBM blend: 3.2×10^{-4}, 2.0×10^{-4} and 3.7×10^{-4} $cm^2 V^{-1} s^{-1}$, respectively. Therefore, the pristine polymer **P1** and the **P1**:[60]PCBM composite represent promising ETL materials for PSCs.

PSCs were fabricated in ITO/HTL/perovskite/ETL/Mg/Ag p-i-n configuration (Fig. 3a), where [60]PCBM, P1 or P1:[60]PCBM (1:1 w/w) blend were used as ETL materials. The hybrid HTL comprised of NiO_x colloidal nanoparticles forming a known inorganic HTL [37] covered with organic PTAA (poly[bis(4-phenyl)(2,4,6-trimethylphenyl)amine]) film was used in combination with the $Cs_{0.12}FA_{0.88}PbI_3$ perovskite absorber. However, a pristine PTAA layer was used as HTL in $MAPbI_3$-based perovskite solar cells.

The open-circuit voltage (V_{OC}), short-circuit current density (J_{SC}), fill factor (FF), and PCE of the optimized devices are presented in Table 1. Among all the investigated fullerene-polymer blends, we provide the

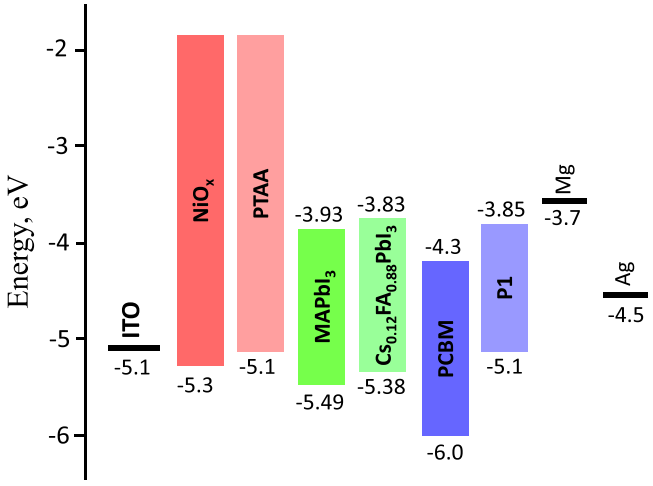

Fig. 1. Energy level diagram of the materials used in PSCs. Band position values are taken from refs [35,36]. Energy levels of $Cs_{0.12}FA_{0.88}PbI_3$ were estimated based on the literature data[3].

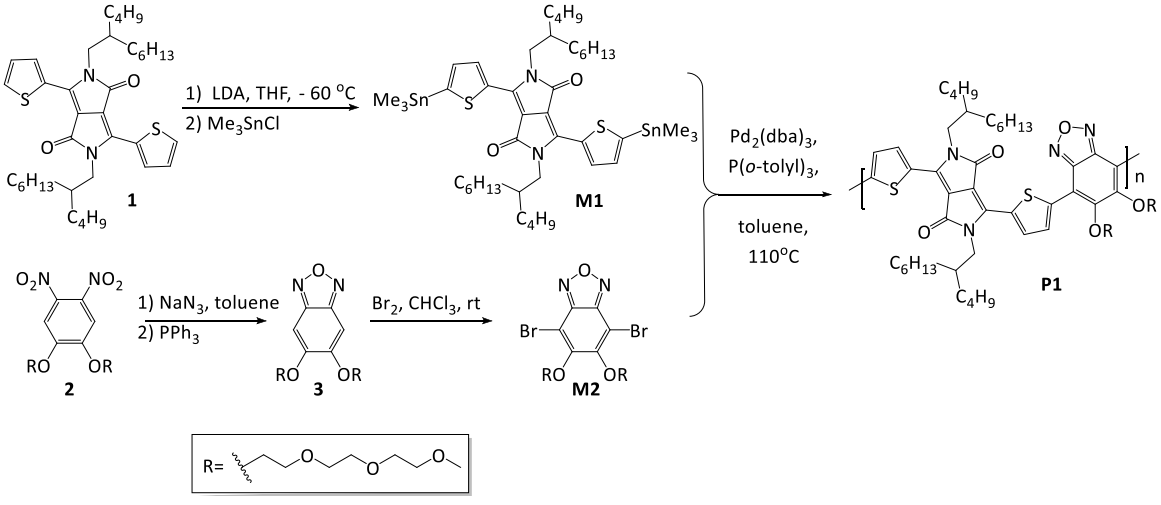

Scheme 1. Synthesis of conjugated polymer **P1**.

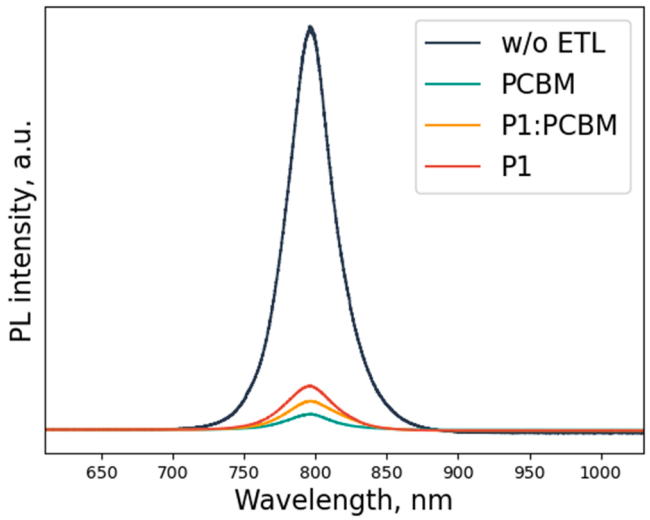

Fig. 2. Photoluminescence spectra of the pristine glass/$Cs_{0.12}FA_{0.88}PbI_3$ films and glass/$Cs_{0.12}FA_{0.88}PbI_3$/ETL stacks, where ETL is represented by [60]PCBM, **P1** or **P1**:[60]PCBM (1:1 w/w) blend.

results for the best-performing composite of P1 with [60]PCBM with the 1:1 wt ratio of the components (data for other ratios are given in SI, Fig. S4).

Fig. 3 shows that polymer P1 and P1:[60]PCBM blend, delivered comparable performances in devices with the pristine [60]PCBM, which is a benchmark ETL material for p-i-n perovskite solar cells. The integration of the external quantum efficiency spectra (EQE) over the reference AM 1.5 G solar spectrum confirmed the J_{SC} values derived from *J*-V measurements. The slope of the *J*-V curve near the open circuit point increases while going from pure PCBM to pure P1, which indicates that incorporating P1 results in a notable increase in the series resistance in the devices. Indeed, the R_s values of 3.6, 6.5 and 3.95 Ω cm^{-2} were extracted from the J-V curves for devices comprising pristine [60]PCBM, P1 or P1:[60]PCBM blend, respectively. An increase in the series resistance when replacing [60]PCBM with P1 apparently leads to a decrease in the device FF from 77% to 62% and the average solar cell efficiency from 16.7% to 12.8%. Therefore, there is substantial room for further improvements by optimizing the structure of P1 to improve its charge transport properties and prevent the extraction of holes from the absorber layer and the associated recombination losses.

We investigated the operational stability of non-encapsulated PSCs with $Cs_{0.12}FA_{0.88}PbI_3$ absorber layer under continuous light soaking (non-filtered light from metal-halide lamps, 30 ± 3 mW/cm^2, 45 ± 2 °C) for 1200 h in an inert nitrogen atmosphere. The efficiency of the reference devices using [60]PCBM as ETL dropped by 45% within the first 100 h of aging (Fig. 4). The PSCs incorporating P1 as ETL showed even faster degradation with about 55% loss in PCE after 100 h. On the contrary, using the composite P1:[60]PCBM as ETL provided remarkably improved stability: the devices lost less than 10% of the initial PCE after 100 h of aging and retained ~ 70% of the original efficiency after 1200 h of continuous light soaking. This is one of the longest lifetimes demonstrated for p-i-n perovskite solar cells assembled using fully organic ETL materials (Table S2, SI).

Very similar results were also obtained for the perovskite solar cells fabricated using $MAPbI_3$ as absorber material. The devices incorporating either [60]PCBM or P1 as ETL degraded severely by losing > 80% of their initial efficiency in the first 24 h under continuous exposure to 100 ± 3 mW/cm^2 white light at 45 ± 2 °C (Fig. S5, SI). On the contrary, the solar cells assembled with P1:[60]PCBM blend as the electron-transport layer were much more stable and lost only 20% of their initial efficiency under the same conditions.

The scanning electron microscopy (SEM) cross-sectional images

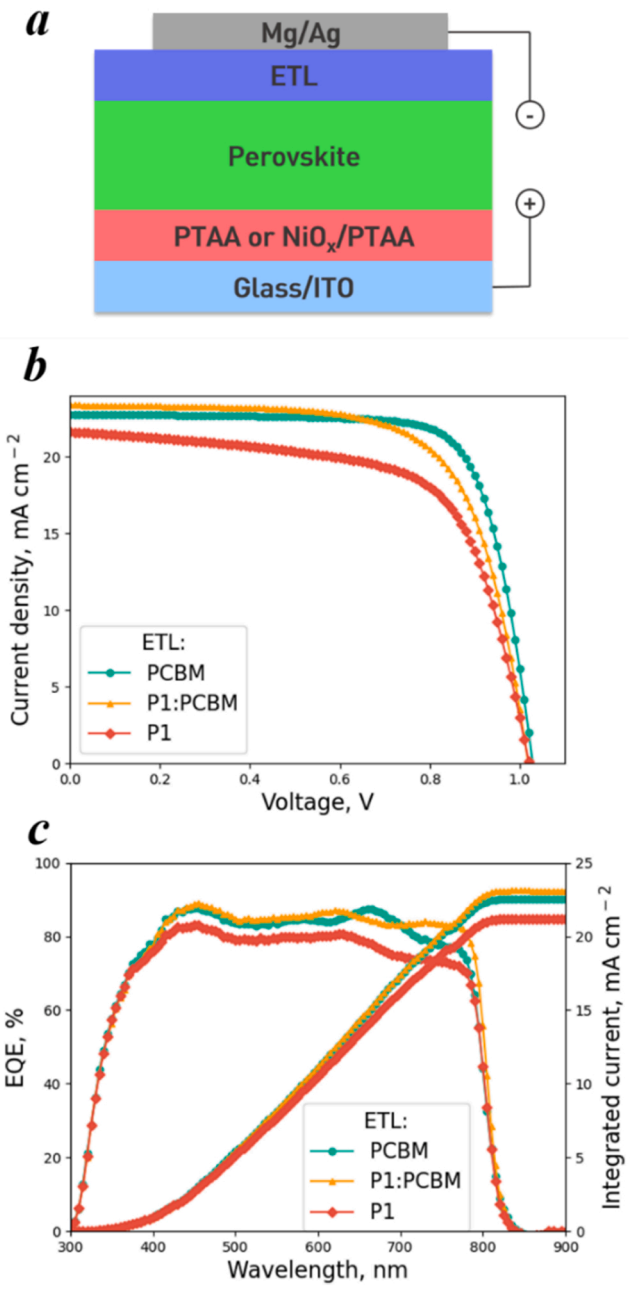

Fig. 3. Schematic layout of perovskite solar cells architecture (a), *J*–V characteristics (b) and EQE spectra (c) of ITO/NiO_x/PTAA/$Cs_{0.12}FA_{0.88}PbI_3$/ETL/Mg/Ag PSCs assembled with different ETL materials.

(Fig. 5a-b) revealed that some voids appear at the perovskite/HTL interface in the case of using [60]PCBM as ETL, which is a known sign of light-induced perovskite degradation [38]. The degradation was the most dramatic for the cells incorporating pure polymer P1 as the ETL: multiple voids appear in the active layer, while the ETL itself shows delamination from the perovskite absorber layer (Fig. 5c-d).

The contact angle measurements performed using diiodomethane as the liquid phase provided the values of 18.9°, 26.1°, and 41.0° for the films of $MAPbI_3$, [60]PCBM, and P1, respectively (Fig. S6, SI). These results confirm that the surface properties of P1 do not match that of the perovskite, so this material is expected to have poor adhesion to the absorber layer, which explains the delamination effect revealed by SEM. Thus, using pristine P1 as ETL material is problematic due to its delamination from the absorber layer.

On the contrary, [60]PCBM has appropriate surface properties and

Table 1
The performance parameters of perovskite solar cells with different ETLs[a].

Perovskite	ETL	Scan direction	V_{OC}[V]	J_{SC} [mA cm^{-2}]	FF [%]	PCE [%]
$Cs_{0.12}FA_{0.88}PbI_3$	[60]PCBM	Forward	1.01 ± 0.01(1.02)	21.5 ± 0.8(22.7)	76.0 ± 1.3(75.6)	16.4 ± 0.8(17.6)
		Reverse	1.01 ± 0.02(1.03)	21.5 ± 0.8(22.7)	77.0 ± 1.6(76.0)	16.7 ± 0.8(17.8)
	P1:[60]PCBM	Forward	1.0 ± 0.02(1.0)	22.3 ± 1.2(23.4)	59.5 ± 1.8(60.0)	13.1 ± 0.7(13.8)
		Reverse	1.01 ± 0.01(1.02)	22.2 ± 1.3(23.4)	67.0 ± 2.2 (68.9)	15.0 ± 0.7 (16.4)
	P1	Forward	0.98 ± 0.02(1.01)	20.4 ± 1.2(21.9)	48.4 ± 5.0(56.0)	9.7 ± 1.4(12.4)
		Reverse	1.0 ± 0.02(1.02)	20.7 ± 1.0(21.6)	62.0 ± 3.0(65.3)	12.8 ± 1.0(14.4)
$MAPbI_3$	[60]PCBM	Forward	1.08 ± 0.02(1.1)	19.6 ± 1.0(20.8)	70.3 ± 2.6(73.0)	15.0 ± 1.4(16.8)
		Reverse	1.1 ± 0.01(1.11)	19.6 ± 1.0(20.7)	71.9 ± 2.4(74.4)	15.5 ± 1.3(17.2)
	P1:[60]PCBM	Forward	1.01 ± 0.02(1.03)	21.1 ± 1.0(22.1)	58.6 ± 3.1(61.7)	12.5 ± 1.5(14.0)
		Reverse	1.02 ± 0.01(1.03)	21.2 ± 1.0(22.2)	60.5 ± 3.4(63.9)	13.1 ± 1.5(14.6)
	P1	Forward	1.02 ± 0.02(1.04)	18.4 ± 1.0(18.8)	55.0 ± 2.4(59.0)	10.2 ± 0.9(11.5)
		Reverse	1.05 ± 0.01(1.06)	18.5 ± 0.5(18.4)	64.0 ± 2.4 (67.4)	12.5 ± 0.5(13.2)

[a] The standard deviation was calculated for a batch of 16 cells tested under forward and reverse scan directions. Values in parentheses are for the best-performing devices.

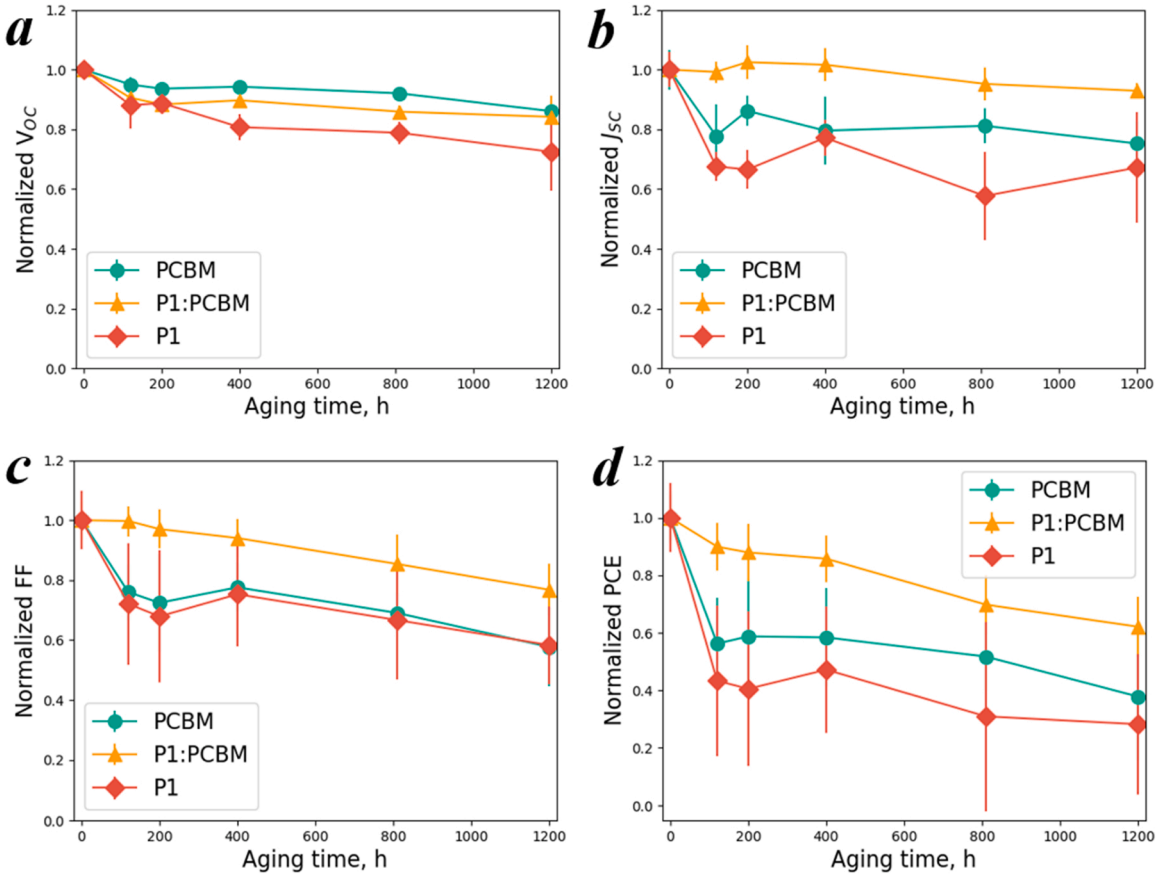

Fig. 4. Operational stability of the ITO/NiO_x/PTAA/$Cs_{0.12}FA_{0.88}PbI_3$/ETL/Mg/Ag perovskite solar cells using P1 (violet), P1:PCBM (orange) and PCBM (green) as ETL materials (30 ± 3 mW/cm^2, 45 ± 2 °C, nitrogen atmosphere). Evolution of the normalized open circuit voltage (a), short circuit current density (b), FF (c) and power conversion efficiency (d) is shown.

does not delaminate from the perovskite films. However, there is another aging pathway realized in this case: the ETL films are not compact enough due to the presence of big cavities in the crystal packing, which are almost unavoidable for the fullerene molecules with their bulky 3D structure. Therefore, the fullerene derivatives such as [60]PCBM support facile diffusion of the methylammonium and iodide species through the electron transport layer, which results in severe corrosion of the top electrode in PSCs as shown previously.[5].

However, both aforementioned aging pathways realized for pristine P1 and [60]PCBM can be efficiently mitigated by using P1:[60]PCBM composites as ETL materials. First, the composite films have the appropriate surface properties, which prevents their delamination from the perovskite absorber. Second, the composite films are expected to have a much more compact structure since the flexible polymer chains (and also their side chains) could fill the cavities between the fullerene spheres. Thus, the composite ETL layer blocks the diffusion of the volatile perovskite aging products to the top electrode and also suppresses the metal diffusion through the ETL to the device active layer.

This hypothesis is well supported by the SEM cross-sectional images of the aged ITO/PTAA/$MAPbI_3$/P1:[60]PCBM/Al cells, which do not reveal any signs of the degradation of the absorber layer or any of the functional interfaces (Fig. 5e-f). The perovskite layer shows a highly-ordered crystalline structure without voids, while the ETL does not undergo any delamination. These findings are consistent with the

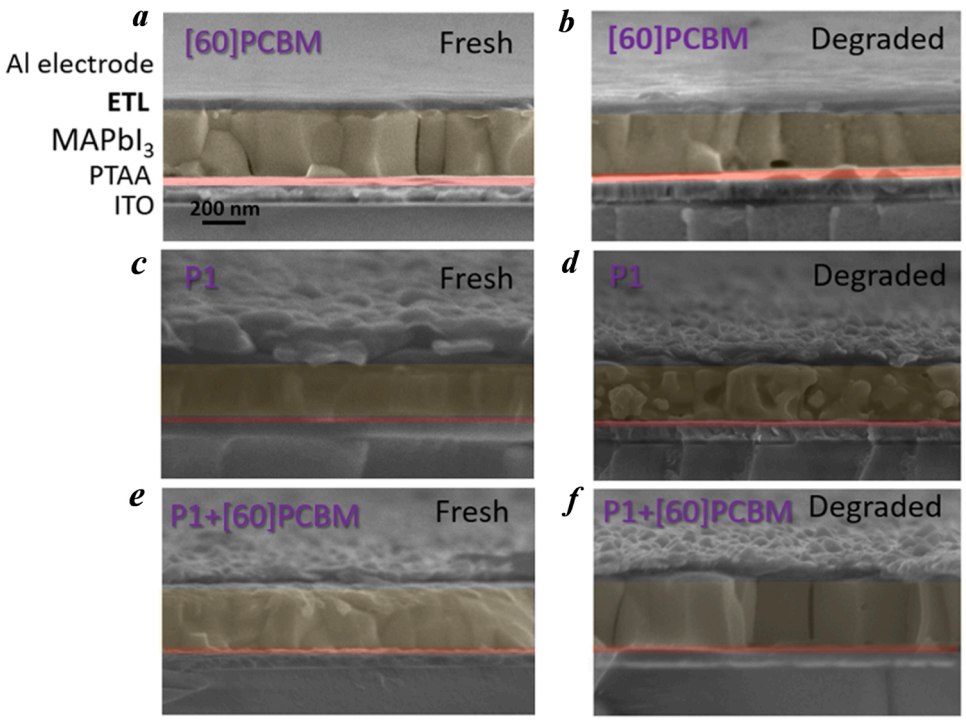

Fig. 5. Cross-sectional SEM images of fresh (a, c, e) and aged (b, d, f) devices using PCBM (a, b), P1 (c, d) and P1:PCBM (e, f) as ETL materials. Aging was performed under continuous 100 ± 3 mW/cm^2 white light exposure at 45 ± 2 °C for 100 h.

superior operational stability of the solar cells using the composite P1:[60]PCBM electron-transport layer as compared to the reference cells with P1 or [60]PCBM used alone.

The additional evidence was provided by the time-of-flight secondary ion mass spectrometry (ToF SIMS) analysis of the aged ITO/PTAA/$MAPbI_3$/P1/Al and ITO/PTAA/$MAPbI_3$/P1 + [60]PCBM/Al device stacks. It has been revealed that P1 does not block interdiffusion of the aluminum top electrode and perovskite active layer components, which undergo strong intermixing after 50 h of aging. On the contrary, P1:[60]PCBM blend has much better diffusion barrier properties and prevents the contact of the aluminum with the perovskite active layer on the same aging timescale (Fig. S7, SI). Thus, ToF SIMS profiles are also consistent with the superior operational stability of the perovskite solar cells incorporating P1:[60]PCBM composite films as ETL.

3. Conclusions

In conclusion, a conjugated polymer P1 and its composites with [60]PCBM delivered decent efficiencies of 13–16% when used as ETL materials in p-i-n PSCs. Importantly, the application of the P1-[60]PCBM composite ETL enabled an impressive improvement in the operational stability of PSCs, which retained ~70% of the initial PCE after 1200 h of continuous light exposure. The obtained results feature the potential of rational design of polymeric ETL materials for efficient and stable p-i-n perovskite solar cells.

CRediT authorship contribution statement

Mohamed Elnaggar: Data Curation, Investigation, Writing – original draft, **Lyubov A. Frolova**: Data Curation, Investigation, Writing – original draft, **Alexandra M. Gordeeva**: Investigation, Writing – original draft, **Marina I. Ustinova**: Investigation, **Hannah Laurenzen**: Investigation, **Alexander V. Akkuratov**: Investigation, **Sergey L. Nikitenko**: Investigation, **Elena A. Solov'eva**: Investigation, **Sergey Yu. Luchkin**: Investigation, **Yury S. Fedotov**: Investigation, **Sergey A. Tsarev**: Investigation, **Nadezhda N. Dremova**: Investigation, **Keith J. Stevenson**: Writing – review & editing, **Sergey I. Bredikhin**: Supervision, **Selina Olthof**: Supervision, Writing – review & editing, **Sergey M. Aldoshin**: Supervision, Funding acquisition, Project administration, **Pavel A. Troshin**: Conceptualization, Methodology, Project administration, Writing – review & editing, Supervision.

Declaration of Competing Interest

The authors declare that they have no known competing financial interests or personal relationships that could have appeared to influence the work reported in this paper.

Acknowledgments

This work was supported by the Russian Science Foundation (project No. 19-73-30020).

Appendix A. Supporting information

Supplementary data associated with this article can be found in the online version at doi:10.1016/j.synthmet.2022.117028.

References

[1] Best Research-Cell Efficiency Chart | Photovoltaic Research | NREL, (n.d.). ⟨https://www.nrel.gov/pv/cell-efficiency.html⟩ (accessed September 24, 2021).
[2] R. Wang, M. Mujahid, Y. Duan, Z. Wang, J. Xue, Y. Yang, A review of perovskites solar cell stability, Adv. Funct. Mater. 29 (2019), 1808843, https://doi.org/10.1002/adfm.201808843.
[3] A.K. Jena, A. Kulkarni, T. Miyasaka, Halide perovskite photovoltaics: background, status, and future prospects, Chem. Rev. 119 (2019) 3036–3103, https://doi.org/10.1021/acs.chemrev.8b00539.
[4] J. Bisquert, E.J. Juarez-Perez, The causes of degradation of perovskite solar cells, J. Phys. Chem. Lett. 10 (2019) 5889–5891, https://doi.org/10.1021/acs.jpclett.9b00613.
[5] A.F. Akbulatov, L.A. Frolova, M.P. Griffin, I.R. Gearba, A. Dolocan, D.A. Vanden Bout, S. Tsarev, E.A. Katz, A.F. Shestakov, K.J. Stevenson, P.A. Troshin, Effect of electron-transport material on light-induced degradation of inverted planar junction perovskite solar cells, Adv. Energy Mater. 7 (2017), 1700476, https://doi.org/10.1002/aenm.201700476.

[6] M. Elnaggar, A.G. Boldyreva, M. Elshobaki, S.A. Tsarev, Y.S. Fedotov, O. R. Yamilova, S.I. Bredikhin, K.J. Stevenson, S.M. Aldoshin, P.A. Troshin, Decoupling contributions of charge-transport interlayers to light-induced degradation of p-i-n perovskite solar cells, Sol. RRL 4 (2020), 2000191, https://doi.org/10.1002/solr.202000191.
[7] Y. Li, Y. Zhao, Q. Chen, Y. (Michael) Yang, Y. Liu, Z. Hong, Z. Liu, Y.T. Hsieh, L. Meng, Y. Li, Y. Yang, Multifunctional fullerene derivative for interface engineering in perovskite solar cells, J. Am. Chem. Soc. 137 (2015) 15540–15547, https://doi.org/10.1021/JACS.5B10614/SUPPL_FILE/JA5B10614_SI_001.PDF.
[8] G. Xu, R. Xue, W. Chen, J. Zhang, M. Zhang, H. Chen, C. Cui, H. Li, Y. Li, Y. Li, New strategy for two-step sequential deposition: incorporation of hydrophilic fullerene in second precursor for high-performance p-i-n planar perovskite solar cells, Adv. Energy Mater. 8 (2018), 1703054, https://doi.org/10.1002/AENM.201703054.
[9] S. Wang, H. Chen, J. Zhang, G. Xu, W. Chen, R. Xue, M. Zhang, Y. Li, Y. Li, S. H. Wang, H.Y. Chen, G.Y. Xu, W.J. Chen, R.M. Xue, M.Y. Zhang, Y.W. Li, Y.F. Li, J. D. Zhang, Targeted therapy for interfacial engineering toward stable and efficient perovskite solar cells, Adv. Mater. 31 (2019), 1903691, https://doi.org/10.1002/ADMA.201903691.
[10] G. Li, R. Zhu, Y. Yang, Polymer solar cells, Nat. Photonics 63 (2012) 153–161, https://doi.org/10.1038/nphoton.2012.11.
[11] Y. Li, Molecular design of photovoltaic materials for polymer solar cells: toward suitable electronic energy levels and broad absorption, Acc. Chem. Res. 45 (2012) 723–733, https://doi.org/10.1021/AR2002446.
[12] S. Wang, Z. Zhang, Z. Tang, C. Su, W. Huang, Y. Li, G. Xing, Polymer strategies for high-efficiency and stable perovskite solar cells, Nano Energy 82 (2021), 105712, https://doi.org/10.1016/J.NANOEN.2020.105712.
[13] L. Yan, C.Q. Ma, Degradation of polymer solar cells: knowledge learned from the polymer: fullerene solar cells, Energy Technol. 9 (2021), 2000920, https://doi.org/10.1002/ENTE.202000920.
[14] K.H. Girish, K.A. Vishnumurthy, T.S. Roopa, Role of conducting polymers in enhancing the stability and performance of perovskite solar cells: a brief review, Mater. Today Sustain. 17 (2022), 100090, https://doi.org/10.1016/J.MTSUST.2021.100090.
[15] N. Sazali, H. Ibrahim, A.S. Jamaludin, M.A. Mohamed, W.N.W. Salleh, M.N. Z. Abidin, A short review on polymeric materials concerning degradable polymers, IOP Conf. Ser. Mater. Sci. Eng. 788 (2020), 012047, https://doi.org/10.1088/1757-899X/788/1/012047.
[16] H. Sun, X. Guo, A. Facchetti, High-performance n-type polymer semiconductors: applications, recent development, and challenges, Chem 6 (2020) 1310–1326, https://doi.org/10.1016/j.chempr.2020.05.012.
[17] P. Zeng, W. Deng, M. Liu, Recent advances of device components toward efficient flexible perovskite solar cells, Sol. RRL 4 (2020), 1900485, https://doi.org/10.1002/solr.201900485.
[18] Z. Yang, B.H. Babu, S. Wu, T. Liu, S. Fang, Z. Xiong, L. Han, W. Chen, Review on practical interface engineering of perovskite solar cells: from efficiency to stability, Sol. RRL 4 (2020), 1900257, https://doi.org/10.1002/solr.201900257.
[19] W. Wang, J. Yuan, G. Shi, X. Zhu, S. Shi, Z. Liu, L. Han, H.Q. Wang, W. Ma, Inverted planar heterojunction perovskite solar cells employing polymer as the electron conductor, ACS Appl. Mater. Interfaces 7 (2015) 3994–3999, https://doi.org/10.1021/am506785k.
[20] S. Shao, Z. Chen, H.H. Fang, G.H. Ten Brink, D. Bartesaghi, S. Adjokatse, L.J. A. Koster, B.J. Kooi, A. Facchetti, M.A. Loi, N-type polymers as electron extraction layers in hybrid perovskite solar cells with improved ambient stability, J. Mater. Chem. A 4 (2016) 2419–2426, https://doi.org/10.1039/c5ta10696f.
[21] Y. Shi, W. Chen, Z. Wu, Y. Wang, W. Sun, K. Yang, Y. Tang, H.Y. Woo, M. Zhou, A. B. Djurišić, Z. He, X. Guo, Imide-functionalized acceptor-acceptor copolymers as efficient electron transport layers for high-performance perovskite solar cells, J. Mater. Chem. A 8 (2020) 13754–13762, https://doi.org/10.1039/d0ta03548c.
[22] W. Chen, Y. Shi, Y. Wang, X. Feng, A.B. Djurišić, H.Y. Woo, X. Guo, Z. He, N-type conjugated polymer as efficient electron transport layer for planar inverted perovskite solar cells with power conversion efficiency of 20.86%, Nano Energy 68 (2020), 104363 https://doi.org/10.1016/j.nanoen.2019.104363.
[23] A.A. Said, J. Xie, Y. Wang, Z. Wang, Y. Zhou, K. Zhao, W. Gao, T. Michinobu, Q. Zhang, Efficient inverted perovskite solar cells by employing N-Type (D–A $_1$ –D–A $_2$) polymers as electron transporting layer, Small 15 (2019), 1803339, https://doi.org/10.1002/smll.201803339.
[24] Z. Zhu, D. Zhao, C.C. Chueh, X. Shi, Z. Li, A.K.Y. Jen, Highly efficient and stable perovskite solar cells enabled by all-crosslinked charge-transporting layers, Joule 2 (2018) 168–183, https://doi.org/10.1016/j.joule.2017.11.006.
[25] J.H. Heo, M. Jahandar, S.J. Moon, C.E. Song, S.H. Im, Inverted CH3NH3PbI3 perovskite hybrid solar cells with improved flexibility by introducing a polymeric electron conductor, J. Mater. Chem. C 5 (2017) 2883–2891, https://doi.org/10.1039/c6tc05081f.
[26] Z. Zhu, C.-C. Chueh, G. Zhang, F. Huang, H. Yan, A.K.-Y. Jen, Improved ambient-stable perovskite solar cells enabled by a hybrid polymeric electron-transporting layer, ChemSusChem 9 (2016) 2586–2591, https://doi.org/10.1002/cssc.201600921.
[27] C. Sun, Z. Wu, H.-L. Yip, H. Zhang, X.-F. Jiang, Q. Xue, Z. Hu, Z. Hu, Y. Shen, M. Wang, F. Huang, Y. Cao, Amino-functionalized conjugated polymer as an efficient electron transport layer for high-performance planar-heterojunction perovskite solar cells, Adv. Energy Mater. 6 (2016), 1501534, https://doi.org/10.1002/aenm.201501534.
[28] Q. Guo, Y. Xu, B. Xiao, B. Zhang, E. Zhou, F. Wang, Y. Bai, T. Hayat, A. Alsaedi, Z. Tan, Effect of energy alignment, electron mobility, and film morphology of perylene diimide based polymers as electron transport layer on the performance of perovskite solar cells, ACS Appl. Mater. Interfaces 9 (2017) 10983–10991, https://doi.org/10.1021/acsami.7b00902.
[29] S. Zuo, X. Zhu, J. Feng, Z. Wang, C. Zhang, C. Wang, X. Ren, S. (Frank) Liu, D. Yang, High-performance inverted perovskite solar cells by reducing electron capture region for electron transport layers, Sol. RRL 3 (2019), 1900207, https://doi.org/10.1002/solr.201900207.
[30] K. Jiang, F. Wu, L. Zhu, H. Yan, Naphthodiperylenetetraimide-based polymer as electron-transporting material for efficient inverted perovskite solar cells, ACS Appl. Mater. Interfaces 10 (2018) 36549–36555, https://doi.org/10.1021/acsami.8b12675.
[31] H. Il Kim, M.-J. Kim, K. Choi, C. Lim, Y.-H. Kim, S.-K. Kwon, T. Park, Improving the performance and stability of inverted planar flexible perovskite solar cells employing a novel NDI-based polymer as the electron transport layer, Adv. Energy Mater. 8 (2018), 1702872, https://doi.org/10.1002/aenm.201702872.
[32] Y. Li, P. Sonar, L. Murphy, W. Hong, High mobility diketopyrrolopyrrole (DPP)-based organic semiconductor materials for organic thin film transistors and photovoltaics, Energy Environ. Sci. 6 (2013) 1684–1710, https://doi.org/10.1039/c3ee00015j.
[33] Y. Li, B. Sun, P. Sonar, S.P. Singh, Solution processable poly(2,5-dialkyl-2,5-dihydro-3,6-di-2-thienyl- pyrrolo[3,4-c]pyrrole-1,4-dione) for ambipolar organic thin film transistors, Org. Electron. 13 (2012) 1606–1613, https://doi.org/10.1016/j.orgel.2012.04.023.
[34] S. Shao, M. Abdu-Aguye, L. Qiu, L.H. Lai, J. Liu, S. Adjokatse, F. Jahani, M. E. Kamminga, G.H. Ten Brink, T.T.M. Palstra, B.J. Kooi, J.C. Hummelen, M. Antonietta Loi, Elimination of the light soaking effect and performance enhancement in perovskite solar cells using a fullerene derivative, Energy Environ. Sci. 9 (2016) 2444–2452, https://doi.org/10.1039/c6ee01337f.
[35] Y. Bai, X. Meng, S. Yang, Interface engineering for highly efficient and stable planar p-i-n perovskite solar cells, Adv. Energy Mater. 8 (2018), 1701883, https://doi.org/10.1002/aenm.201701883.
[36] Y. Jiang, M.R. Leyden, L. Qiu, S. Wang, L.K. Ono, Z. Wu, E.J. Juarez-Perez, Y. Qi, Combination of hybrid CVD and cation exchange for upscaling Cs-substituted mixed cation perovskite solar cells with high efficiency and stability, Adv. Funct. Mater. 28 (2018), 1703835, https://doi.org/10.1002/adfm.201703835.
[37] J.-Y. Jeng, K.-C. Chen, T.-Y. Chiang, P.-Y. Lin, T.-D. Tsai, Y.-C. Chang, T.-F. Guo, P. Chen, T.-C. Wen, Y.-J. Hsu, Nickel oxide electrode interlayer in CH3NH3PbI3 perovskite/PCBM planar-heterojunction hybrid solar cells, Adv. Mater. 26 (2014) 4107–4113, https://doi.org/10.1002/ADMA.201306217.
[38] L.A. Frolova, A.I. Davlethanov, N.N. Dremova, I. Zhidkov, A.F. Akbulatov, E. Z. Kurmaev, S.M. Aldoshin, K.J. Stevenson, P.A. Troshin, Efficient and stable MAPbI3-based perovskite solar cells using polyvinylcarbazole passivation, J. Phys. Chem. Lett. 11 (2020) 6772–6778, https://doi.org/10.1021/ACS.JPCLETT.0C01776.